DISPLACEMENT AND DEFLECTION OF AN OPTICAL BEAM BY AIRBORNE ULTRASOUND

James N. Caron*†

*Research Support Instruments, 4325-B Forbes Boulevard,
Lanham, MD 20706
†Quarktet, 205 Indian Spring Drive, Silver Spring, MD 20901

ABSTRACT. Gas-Coupled Laser Acoustic Detection enables laser-based sensing of ultrasound from a solid without contact of the surface, and independent of the optical properties of the solid surface. The interaction between the probe beam and acoustic field has typically been modeled as creating a deflection in the optical beam. This paper describes this interaction as a combination of displacement and deflection. Sensing displacement can significantly decrease the system's dependence of length.

Keywords: Laser-based Ultrasound, Optical Beam Deflection, Optical Beam Displacement
PACS: 42.15.Eq, 42.62.Cf, 42.79.Jq, 43.58.+z

INTRODUCTION

Gas-coupled Laser Acoustic Detection, [1–5] or GCLAD, is a non-contact acoustic sensor that enables laser-based detection of ultrasound in materials. A probe laser beam is directed parallel to, but does not contact the sample surface. The optical path is diverted by changes in the index of refraction created by the acoustic wave emanating from the sample surface. As depicted in Figure 1, the change in path is detected by a split-cell position-sensitive photodetector. In contrast to other laser-based ultrasound detection techniques [6–10], this method is independent of the optical properties of the sample surface.

In previous papers, the interaction between the laser and airborne ultrasound has been described as a deflection of the beam from the optical path. [1, 2] However, laboratory tests have shown that the interaction cannot be solely explained by a deflection. In this study, the resulting GCLAD signal is shown to be a combination of the deflection and a displacement of the optical beam by the acoustic field, shown pictorially in Figure 2. The term displacement is used here to describe two deflections that result in a displaced beam. For optical deflection, sensitivity increases as the distance between the acoustic disturbance and detector is increased. This is limited by the divergence of the optical beam, producing an upper limit on the sensitivity. The use of the displacement signal is advantageous since it diminishes the dependence of the system on the distance between the ultrasonic interaction and the detector.

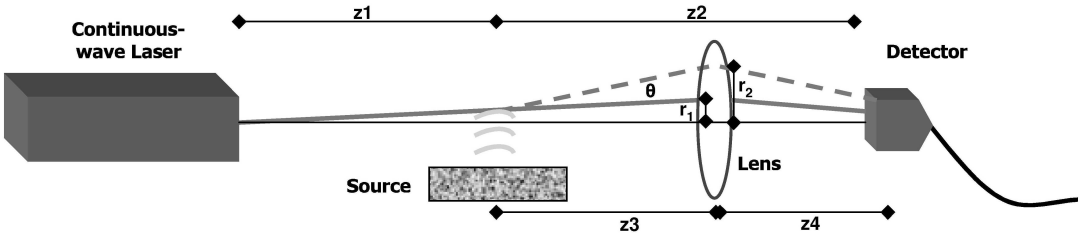

FIGURE 1: Arrangement for the sensing of laser-generated ultrasonic waveforms with GCLAD. Ultrasonic waveforms, upon transmission through the material, radiate an airborne wave. This modulates the index of refraction transverse to the probe beam and causes a change in the direction of the optical beam path. The change is detected by a position-sensitive photodetector.

FIGURE 2: (Left) The deflection of an optical beam by an acoustic field. (Right) Two deflections in the acoustic field create an optical displacement of the beam.

THEORY

The GCLAD signal is modeled as a combination of the response to a displacement and a deflection of the optical beam. Both actions cause a displacement of the laser beam on a split-cell position-sensitive photodetector. The response of the photodetector to this movement is derived in the following section. The dependence of beam width as a function of distance is then calculated with and without a lens in the optical path. Finally, the signal resulting from the displacement and deflection of the beam by an acoustic pulse is derived.

Detection of Laser Beam Deflection

The acoustic signal is detected by the displacement of the laser beam on the photodetector. Let the probe laser power density (i.e. irradiance) equal

$$I(r) = \frac{P_o}{\pi \omega_D^2} e^{-(r/\omega_D)^2} \tag{1}$$

such that

$$P_o \equiv 2\pi \int_0^\infty I(r) r \, dr \tag{2}$$

is the average power of the laser beam and ω_D is the beam width at the detector.

The detector consists of a dual-element photodiode and customized electronics. The total signal voltage is the difference of the voltages from the two photocells or

$$V_{tot}(\Delta x) = G(V_+(\Delta x) - V_-(\Delta x)) \tag{3}$$

where G is the gain of the amplifier and Δx is the displacement of the beam on the detector. The signal voltage for each photocell is proportional to the light power density

integrated over the area of the photocell. The sensitivity of the photocell can be expressed as

$$\kappa = q\eta/h\nu \tag{4}$$

where q is the electronic charge, η is the quantum efficiency, h is Planck's constant, and ν is the frequency of light. [12]

For a single diode of rectangular geometry, the received voltage is

$$\begin{aligned} V_+(\Delta x) &= R\kappa \int I(x,y)\,dx\,dy \\ &= \frac{R\kappa P_o}{\pi\omega_D^2}\int_{t_c/2}^{d_c/2}\int_{-d_c/2}^{d_c/2} e^{-((x-\Delta x_D)/\omega_D)^2} e^{-(y/\omega_D)^2}\,dx\,dy \\ &= \frac{2R\kappa P_o}{\pi}\mathrm{erf}\left(\frac{\mathrm{d_c}}{2\omega_\mathrm{D}}\right)\left[\mathrm{erf}\left(\frac{\mathrm{d_c}-2\Delta\mathrm{x_D}}{2\omega_\mathrm{D}}\right)-\mathrm{erf}\left(\frac{\mathrm{t_c}-2\Delta\mathrm{x_D}}{2\omega_\mathrm{D}}\right)\right] \end{aligned} \tag{5}$$

where R is the resistance value that converts the current to a voltage, t_c is the separation distance between the two photocells, and d_c is the diameter of the photocell.

Similarly,

$$V_-(\Delta x) = \frac{2R\kappa P_o}{\pi}\mathrm{erf}\left(\frac{\mathrm{d_c}}{2\omega_\mathrm{D}}\right)\left[\mathrm{erf}\left(\frac{\mathrm{d_c}+2\Delta\mathrm{x_D}}{2\omega_\mathrm{D}}\right)-\mathrm{erf}\left(\frac{\mathrm{t_c}+2\Delta\mathrm{x_D}}{2\omega_\mathrm{D}}\right)\right] \tag{6}$$

The total voltage that results from a displacement of Δx on the photocell is

$$\begin{aligned} V_{tot}\quad (\Delta x) &= \frac{2GR\kappa P_o}{\pi}\mathrm{erf}\left(\frac{\mathrm{d_c}}{2\omega_\mathrm{D}}\right) \\ \times\quad &\left[\mathrm{erf}\left(\frac{d_c-2\Delta x_D}{2\omega_D}\right)-\mathrm{erf}\left(\frac{t_c-2\Delta x_D}{2\omega_D}\right)-\left(\frac{d_c+2\Delta x_D}{2\omega_D}\right)+\mathrm{erf}\left(\frac{t_c+2\Delta x_D}{2\omega_D}\right)\right]. \end{aligned} \tag{7}$$

This equation has the form

$$V(\alpha) = K\left[\mathrm{erf}(\beta-\alpha)-\mathrm{erf}(\beta+\alpha)+\mathrm{erf}(\gamma+\alpha)-\mathrm{erf}(\gamma-\alpha)\right] \tag{8}$$

where K is a constant, $\alpha \equiv \Delta x_D/\omega_D$, $\beta \equiv d_c/2\omega_D$, and $\gamma \equiv t_c/2\omega_D$.

The erf function can be expanded as a Taylor series expansion [14] around β and γ to produce

$$\begin{aligned} V(\alpha) &\cong K[\mathrm{erf}(\beta)+(\beta-\alpha)\mathrm{erf}'(\beta)-\mathrm{erf}(\beta)-(\beta+\alpha)\mathrm{erf}'(\beta)+\mathrm{erf}(\gamma) \\ &+ (\gamma+\alpha)\mathrm{erf}'(\gamma)-\mathrm{erf}(\gamma)-(\gamma-\alpha)\mathrm{erf}'(\gamma)] \\ &\cong \frac{-4K\alpha}{\sqrt{\pi}}\left[e^{-\beta^2}-e^{-\gamma^2}\right] \end{aligned} \tag{9}$$

or with substitution

$$V_{tot}(\Delta x) \approx \frac{-8GR\kappa P_o}{\sqrt{\pi^3}}\mathrm{erf}\left(\frac{\mathrm{d}}{2\omega_\mathrm{D}}\right)\frac{\Delta\mathrm{x}}{\omega_\mathrm{D}}\left[\mathrm{e}^{-\mathrm{d_c^2}/4\omega_\mathrm{D}^2}-\mathrm{e}^{-\mathrm{t_c^2}/4\omega_\mathrm{D}^2}\right] \tag{10}$$

For this level of approximation, the received signal is proportional to Δx.

To evaluate this expression further, the dependence of ω_D and Δx on optical path length are determined in the next sections.

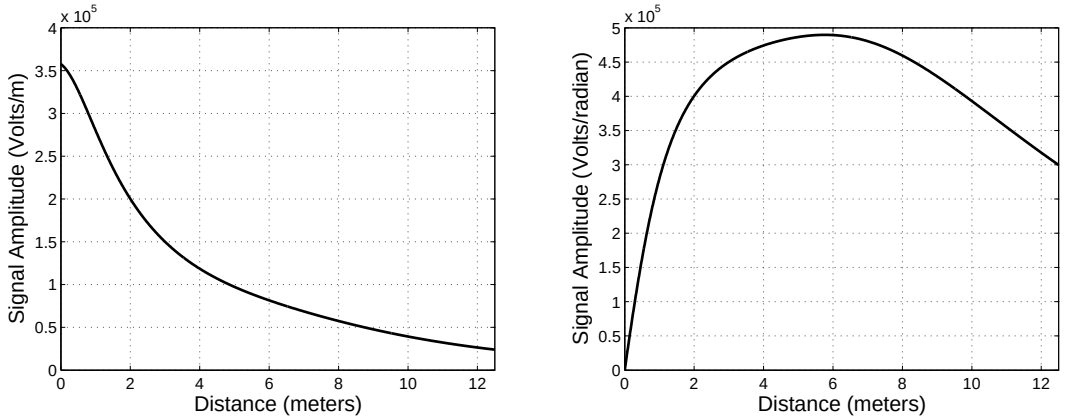

FIGURE 3: (Left) The response of the signal voltage to a unit displacement of the detection beam created by the ultrasound as a function of z_2. (Right) The response of the signal voltage to a unit deflection of the detection beam created by the ultrasound.

Beam Expansion with no Lenses

With no lenses in the setup, the displacement on the detector created by a deflection at $z = z_1$ is simply $\Delta x = z_2\theta$. The displacement at the detector created by a displacement of the beam is $\Delta x = \Delta x_o$. The beam width w expands as a function of distance according to

$$w(z) = w_o\sqrt{1 + \left(\frac{\lambda z}{\pi w_o^2 n}\right)^2} \tag{11}$$

where w_o is the original waist of the beam, z is the distance along the optical path, λ is the wavelength of light, and n is the index of refraction. [13]

Figure 4 shows the response of the photodetector to a unit displacement $V_{tot}(z)/\Delta x_o$ (left) or deflection $V_{tot}(z)/\theta$ (right) of the beam created by the ultrasound. For the calculation and following experiment, the values $P_0 = 133$ mW, $\eta = 0.23$ Amps/Watt, $\lambda = 532$ nm, $t_c = 0.25$ mm, $\omega_o = 0.48$ mm, $R = 131$ ohms, $G = 75$, $d_c = 9.5$ mm are used. Without knowledge of the strengths of the deflection and displacement, no determination of overall signal strength can estimated. However, the plots do reveal information about the maximum signal and relative strength for each case.

Expansion of an Optical Beam through a Single Lens

The divergence of the laser beam as it passes through various optics can be calculated using the ABCD rule. [12] The beam waist is given by

$$w(z_4) = w_0\sqrt{\frac{A_T^2 + B_T^2/s^2}{A_T D_T - B_T C_T}} \tag{12}$$

where $s \equiv \lambda/(\pi\omega_o^2 n)$. The components are calculated using the transfer matrix,

$$\begin{aligned}\begin{pmatrix} A_T & B_T \\ C_T & D_T \end{pmatrix} &= \begin{pmatrix} 1 & z_4 \\ 0 & 1 \end{pmatrix}\begin{pmatrix} 1 & 0 \\ -1/f & 1 \end{pmatrix}\begin{pmatrix} 1 & z_1+z_3 \\ 0 & 1 \end{pmatrix} \\ &= \begin{pmatrix} 1 - z_4/f & z_1 + z_3 + z_4 - z_4(z_1+z_3)/f \\ -1/f & 1 - (z_1+z_3)/f \end{pmatrix}\end{aligned} \tag{13}$$

where $z_1 + z_3$ is the distance from the minimum beam waist (the laser) to the lens.

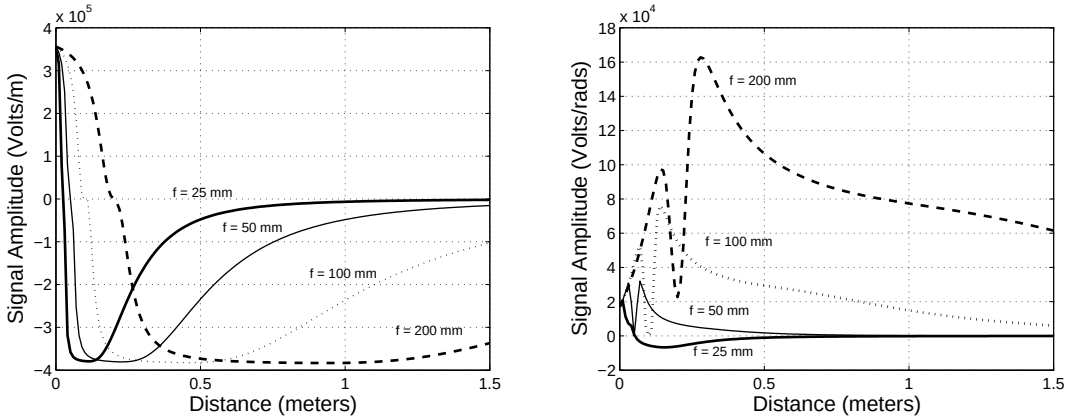

FIGURE 4: (Left) The response of the signal voltage to a unit displacement of the detection beam when sent through a convex lens with focal length f. (Right) The response of the signal voltage to a unit deflection of the detection beam. The scale x-scale corresponds to the z_4 value.

Optical Beam Path Change with a Single Lens

For a single lens of focal length f, the system matrix is [12]

$$A = \begin{pmatrix} 1 - z_4/f & +z_3 + z_4 - z_4 z_3/f \\ -1/f & 1 - (z_1 + z_3)/f \end{pmatrix} \tag{14}$$

The translational change Δx_d and angular change $\Delta\theta_d$ at the detector resulting from a small deflection θ at the interaction point is

$$\begin{pmatrix} \Delta x_d \\ \Delta\theta_d \end{pmatrix} = \begin{pmatrix} 1 - z_4/f & z_3 + z_4 - z_4 z_3/f \\ -1/f & 1 - (z_1 + z_3)/f \end{pmatrix} \begin{pmatrix} 0 \\ \theta \end{pmatrix} \tag{15}$$

producing

$$\Delta X(z) \approx z_4\theta + z_3\theta\left(1 - \frac{z_4}{f}\right) \tag{16}$$

The change at the detector created by a displacement at the interaction point is

$$\begin{pmatrix} \Delta x_c \\ \Delta\theta_c \end{pmatrix} = \begin{pmatrix} 1 - z_4/f & z_3 + z_4 - z_4 z_3/f \\ -1/f & 1 - (z_1 + z_3)/f \end{pmatrix} \begin{pmatrix} \Delta x_o \\ 0 \end{pmatrix} \tag{17}$$

producing

$$\Delta X(z) \approx \Delta x_o(1 - z_4/f) \tag{18}$$

Figure 4 shows the displacement and deflection responses when a lens is placed $z_3 = 5$ cm for different focal lengths. With the lens, the signal created by the deflection is reduced by at least a factor of ten compared to Figure 2. In contrast, the displacement response is slightly higher, and the position of maximum sensitivity can be chosen by changing the focal length of the lens.

COMBINATION WAVEFORM

The displacement and deflection waveforms can have different shapes, interfering constructively or non-constructively. Since their amplitudes vary differently as a function

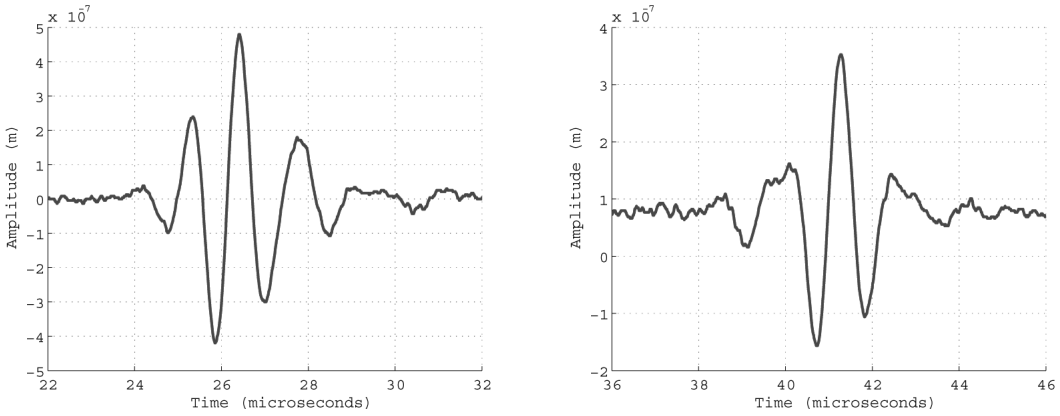

FIGURE 5: Two examples of waveforms captured with the detector placed very close to the interaction point. These waves are used as an approximation to $x(t)$ in Equation 20.

of distance, the received waveform will then change shape as a function of distance. The received waveform $V(z,t)$ is expressed as a combination of waveforms,

$$V(z,t) = A(z)\Delta x(t) + B(z)\theta(t) \tag{19}$$

where $A(z)$ describes how the amplitude of the displaced waveform changes with distance, and $B(z)$ describes how the deflected waveform changes. The function $A(z)$ is created by setting $\Delta x = z_4\theta$ and Equation 11 into Equation 7. Function $B(z)$ uses $\Delta x_d = \Delta z_o$.

To test this empirically, the function $V(z,t)$ can sampled by measuring waveforms at different distances. The functions $A(z)$ and $B(z)$ can be calculated from theory. We assume that close to the interaction, $V_\theta(0,t)$ is significantly small compared to $V_{\Delta x}(0,t)$, such that the waveform is mostly created by displacement of the beam. This produces $\Delta x(t) \approx V_{\Delta x}(0,t)/A(0)$, with examples shown in Figure 5. The function $\theta(t)$ can then be calculated from

$$\theta(t) \approx \frac{V(z,t) - A(z)\Delta x(t)}{B(z)}. \tag{20}$$

If $\theta(t)$ is calculated at different z_4 values, the resulting waveforms should not vary significantly.

This concept was first tested, with no lens and $z_2 = z_4$, by gradually increasing the distance between the photodetector and the detection point, along the $\hat{z}$ axis. The ultrasound source was a 1 MHz contact transducer placed about 13 mm from the laser beam.

Figure 6(Left) shows the $V(z,t)$ waveforms where a change in shape can be noticed. This is an indication that there is mixing occurring between two types of waveforms. Application of Equation 20 produces the waveforms in Figure 6(Right). The first portion of the waveforms are very consistent, being relatively independent on the variation in distance. There is more variation in the second and third peaks.

The experiment was repeated using a $f = 50$ mm convex lens placed at $z_3 = 50$ mm. The transducer was 6 mm from the laser beam. The captured waveforms are shown in Figure 7(Left) and the $\theta(t)$ waveforms are shown in Figure 7(Right). The processed waveforms generally possess the same shape, suggesting that the displacement waveform was successfully subtracted out. The waveforms do exhibit a significant dependence on

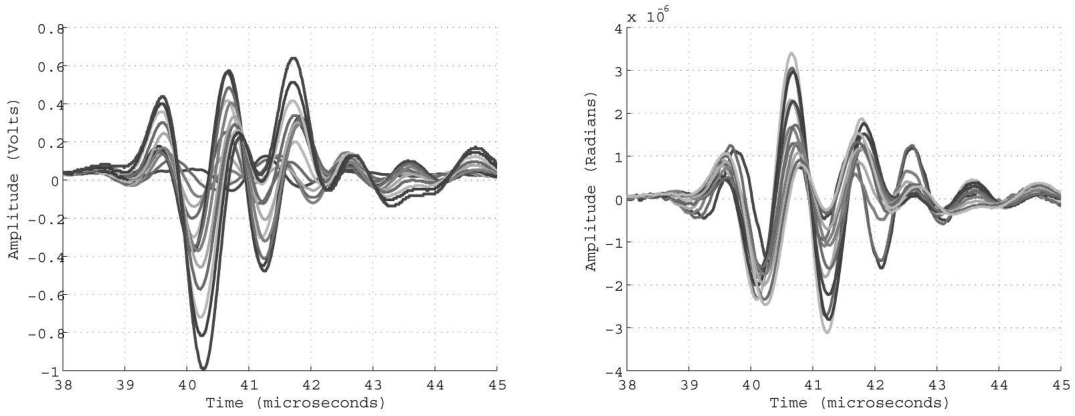

FIGURE 6: (Left) A series of waveforms captured as a function of increasing z_2. The change in change is indicative of a competing set of waveforms. (Right) The result of applying Equation 20 to the captured waves. The amplitudes are generally independent of the distance, indicating that this the waveform created by the deflection of the beam by the ultrasound.

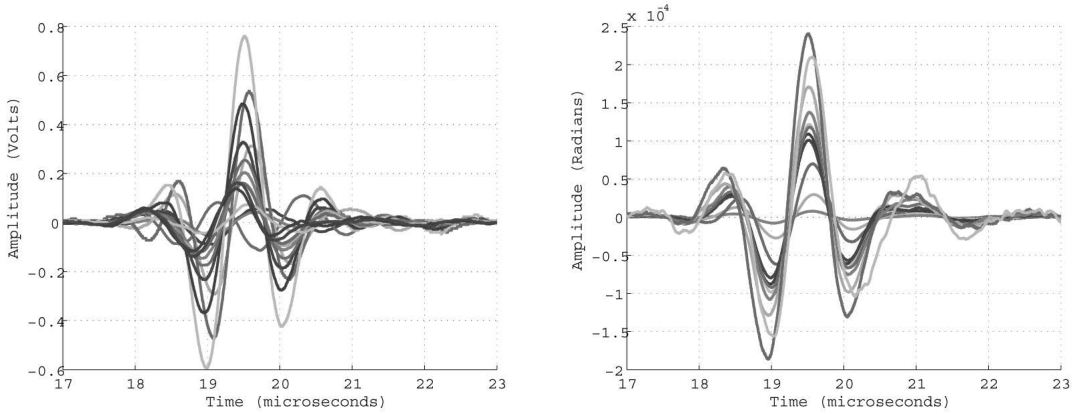

FIGURE 7: (Left) Waveforms captured as a function of distance where a 50 mm lens was placed between the ultrasound and the detector. (Right) Using Equation 20, the $\theta(t)$ component was calculated for $f = 50$ mm. Most of the peaks have similar amplitudes.

distance. In later research, we will examine whether this is caused by $\Delta x(t)$ containing a portion of the deflection wave, or perhaps focusing of the beam by the ultrasound waveform.

This analysis also produces a quantitative estimate of the deflection and displacement values. Figure 6 shows a maximum deflection on the order of 3 microradians. In contrast, Figure 7 shows deflections on the order of 250 microradians. However, in the latter case, the laser beam was closer which may have produced a much stronger deflection. For displacement, $\Delta x(t)$ reaches 0.6μm in the former case, and 0.3μm in the latter.

CONCLUSIONS

The research shows that the interaction of an optical beam with an airborne ultrasound waveform creates both a displacement and a deflection of the beam. Using Gaussian optical theory, the detector signal was modeled for the response to a unit displacement

or deflection. This concept was tested empirically by capturing waveforms as a function of distance both with and without a convex lens. The deflection waveforms, derived from the calculation for each position, exhibited similar shapes, and in the case of no lens, similar amplitudes, affirming the theory. For one lens, the deflection waveforms exhibit an increase in amplitude with distance.

The existence of a displacement waveform allows the GCLAD system to be built on a much smaller scale. Using the analysis described here, GCLAD can be designed with multiple lenses to enhance or diminish the displacement waveform, to separate out the waveforms, or to miniaturize the system.

REFERENCES

1. J.N Caron, Y. Yang, J.B. Mehl and K.V. Steiner, "Gas-coupled Laser Acoustic Detection at Ultrasonic and Audible Frequencies," *Review of Scientific Instruments*, **69(8)**, pp. 2909-2911 (1998).
2. J.N Caron, Y. Yang, J.B. Mehl and K.V. Steiner, "Gas coupled laser acoustic detection for ultrasound inspection of composite materials," *Materials Evaluation*, pp. 667-671, **58**(5) (2001).
3. Caron, J.N., Mehl, J.B., and Steiner, K.V., "Gas-coupled Laser Acoustic Detection," US Patent No. 6 041 020 (March 21, 2000).
4. J.N Caron, Y. Yang, J.B. Mehl and K.V. Steiner, "Overview: Ultrasound sensing using Gas-coupled Laser Acoustic Detection," *Nondestructive Testing and Evaluation*, **17**, pp. 169-177 (2002).
5. J.N. Caron, D.M. Huber, V. DiPietro, and C.J. Rollins, "Progress towards a portable laser-based ultrasound sensor using gas-coupled laser acoustic detection," *Review of Progress in Quantitative Nondestructive Evaluation* , **24A**, edited by D.O. Thompson and D.E. Chimenti, AIP Conference Proceedings vol. 760, American Institute of Physics, Melville, NY, pp. 281-288 (2005).
6. C.B. Scruby and L.E. Drain, *Laser Ultrasonics*, (Adam Hilger: Bristol), 1990.
7. J.W. Wagner, and J.B. Spicer, "Theoretical noise-limited sensitivity of classical interferometry," *Journal of the Optical Society if America B*, **4**(8), pp. 1316-1326, (1987).
8. J.P. Monchalin, *Applied Physics Letters*, **47**, pp. 14-16, (1985).
9. J.P. Monchalin, "Laser-ultrasonics: from the laboratory to industry," *Review of Progress in Quantitative Nondestructive Evaluation*, **23A**, eds. D. O. Thompson and D. E. Chimenti, AIP Conference Proceedings, vol. 700, American Institute of Physics, Melville, NY, pp. 3-31 (2004).
10. I. Lahiri, L.J. Pyrak-Nolte, D.D. Nolte, M.R. Melloch, R.A. Kruger, G.D. Bacher, and M.B. Klein, M. B., "Laser-based ultrasound detection using photorefractive quantum wells," *Applied Physics Letters*, **73(8)**, pp. 1041-1043 (1998)
11. A. Garcia-Valenzuela, "Limits of different schemes used in the optical beam deflection method," *Journal of Applied Physics*, **82(3)**, pp. 985-988 (1997).
12. A. Yariv, *Optical Electronics*, Saunders College Publishing, Philadelphia (1991).
13. J. Alda, "Laser and Gaussian Beam Propagation and Transformation," *Encylcopedia of Optical Engineering*, p. 999 (2003).
14. E.W. Weisstein, "Erf." from MathWorld–A Wolfram Web Resource. http://mathworld.wolfram.com/Erf.html